AIP ADVANCES **3**, 012103 (2013)

Single-order operation of lamellar multilayer gratings in the soft x-ray spectral range

Robert van der Meer,[1,a] Igor Kozhevnikov,[2] Balachander Krishnan,[1] Jurriaan Huskens,[1] Petra Hegeman,[3] Christian Brons,[3] Boris Vratzov,[1,4] Bert Bastiaens,[1] Klaus Boller,[1] and Fred Bijkerk[1,5]
[1]*MESA+ Institute for Nanotechnology, University of Twente, 7522 NB, The Netherlands*
[2]*Institute of Crystallography, Russian Academy of Sciences, 119333, Moscow, Russia*
[3]*PANalytical, Almelo, 7602 EA, The Netherlands*
[4]*NT&D Nanotechnology & Devices, Aachen, 52062, Germany*
[5]*nSI, FOM-Institute DIFFER, formerly Rijnhuizen, Nieuwegein, 3430 BE, The Netherlands*

(Received 28 June 2012; accepted 20 December 2012; published online 2 January 2013)

We demonstrate single-order operation of Lamellar Multilayer Gratings in the soft x-ray spectral range. The spectral resolution was found to be 3.8 times higher than from an unpatterned multilayer mirror, while there were no significant spectral side-band structures adjacent to the main Bragg peak. The measured spectral bandwidths and peak reflectivities were in good agreement with our theoretical calculations. [http://dx.doi.org/10.1063/1.4774297]

In the soft x-ray (SXR) wavelength range, the reflectivity response of multilayer (ML) mirrors is basically narrowband due to the Bragg reflection process, i.e. such mirrors are wavelength selective. This is of high relevance for applications where soft x-rays are to be filtered or monochromatized. An important example is X-ray fluorescence analysis, where the chemical specificity and sensitivity of the method increases with the spectral resolution $E/\Delta E$ of the analyzer, e.g. a Bragg crystal or ML mirror. Unfortunately, the spectral resolution of ML mirrors is fundamentally limited by the inherent absorption of all materials in this wavelength range. More specifically, the absorption limits the penetration depth and thus the number of bi-layers (N_{eff}) effectively contributing to Bragg reflection.[1]

The penetration depth can be increased by removing part of the absorptive material from the ML mirrors by etching a grating into the multilayer structure, resulting in a so-called Lamellar Multilayer Grating (LMG, see Figure 1).[2–6] So far, the best LMGs for the SXR range have reached resolution improvements of a factor of 2.5.[3] However, this is offset by a fundamental loss in reflectivity caused by undesired diffraction by the grating structure. In a simple ML mirror all of the output is in a single beam of zeroth order. However, as is depicted in Figure 1, an LMG diffracts an incident monochromatic plane wave into a number of different diffraction orders, thereby reducing the efficiency for each individual order. This effect is seen in almost all LMGs realized so far and has caused diffraction losses between at least 40 % to more than 85 %.[3,4]

In order to reduce these diffraction losses, in previous work we have identified an operating regime for LMGs, which we call single-order operation.[5,6] The main difference with standard LMG operation is a reduction of the grating period D, and thus lamel width ΓD (see Figure 1). Below a certain grating period, given by:

$$\Gamma D \Delta\theta_{MM} << d, \tag{1}$$

the higher diffraction orders fall out of the acceptance angle, $\Delta\theta_{MM}$, for Bragg reflection by the ML mirror. The incident beam then effectively only excites a single diffraction order, thereby

[a]Author to whom correspondence should be addressed. Electronic mail: r.vandermeer@utwente.nl

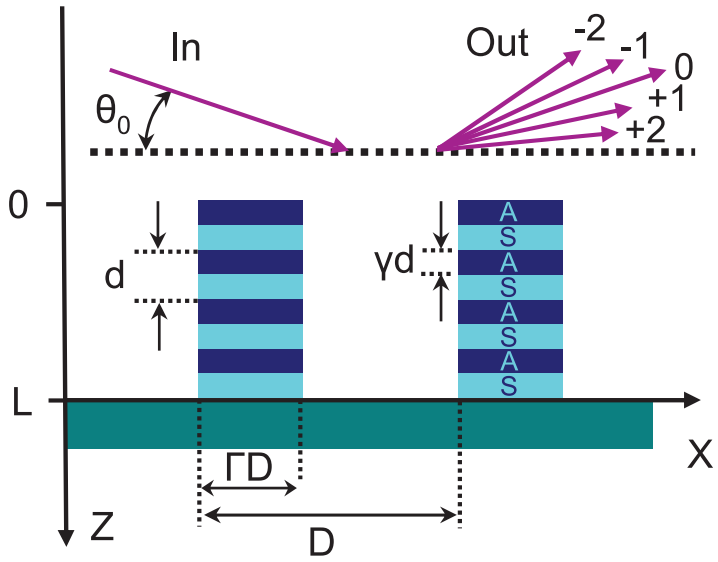

FIG. 1. Schematic cross section of an LMG. An incident beam from the left (In), under grazing angle Θ_0, is reflected from the multilayer and diffracted into multiple orders (Out) by the multilayer structure. The multilayer is built up from N bi-layers (thickness d) consisting of an absorber (A) and spacer material (S) with thickness-ratio γ. The grating structure is defined by the period D and lamel width ΓD (i.e., $\Gamma < 1$ is the ratio of the lamel width to the grating period).

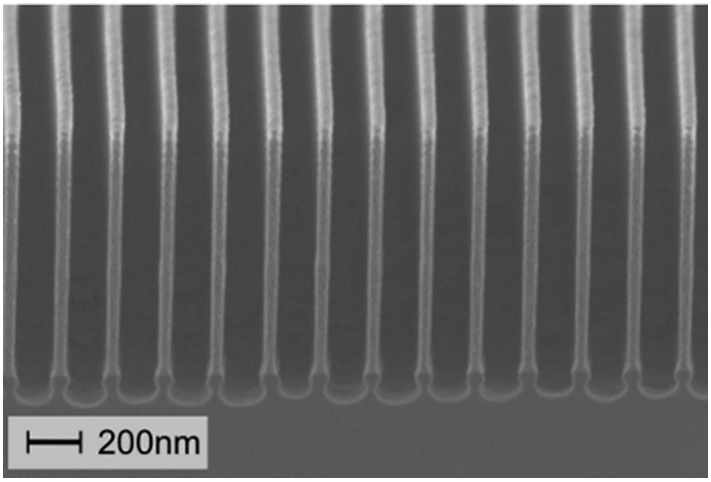

FIG. 2. Scanning Electron Microscope (SEM) image of an LMG with a 200 *nm* grating period and a 60 *nm* lamel width etched into a 1 μm W/Si ML stack.

fundamentally improving LMG reflectivity. In the approximation of a semi-infinite and strictly periodic ML stack, single-order operation improves the spectral resolution by a factor $1/\Gamma$ while the peak reflectivity is maintained in comparison to conventional ML mirrors.[5]

From Eq. (1) we determine that single-order LMG operation in the SXR range requires grating periods and lamel widths well below feature sizes and accuracies previously reported in literature.[3] To overcome these fabricational limitations, we have developed a fabrication process based on UV-nanoimprint lithography and standard Bosch Deep Reactive Ion Etching as described in more detail in Ref. 7. Using this process, we have successfully and reproducibly etched gratings in 1 μm high ML stacks with grating periods down to the required 200 *nm* and lamel widths as narrow as 60 *nm* as is shown in Figure 2.[7]

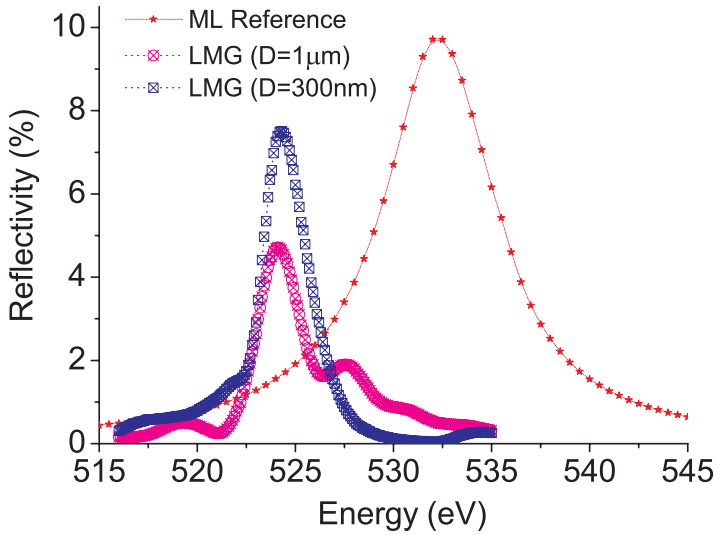

FIG. 3. Experimental reflectivity for two LMGs with the same Γ-ratio of 0.4, operating in the multi-order ($D = 1\ \mu m$) and single-order ($D = 0.3\ \mu m$) regime. The reflectivity of an unpatterned ML mirror is also shown for reference. The lines are guides to the eye.

We report on the first experimental demonstration of single-order LMG operation in the SXR spectral range. Single-order operation also resulted in a record improvement of spectral resolution, here a factor of nearly four as compared with the corresponding unpatterned ML mirror.

To investigate whether single-order LMG operation can be obtained in the SXR spectral range, we fabricated several LMGs with various combinations of grating periods (D), lamel widths (ΓD) and Γ-ratios. The grating dimensions were chosen between 200 and 2000 *nm* with Γ-ratios between 0.2 and 1. This enabled us to perform a systematic investigation of single- and multi-order operation as function of the grating parameters for SXR energies between 500 and 1500 *eV*. The LMGs were fabricated in a commercially obtained ML mirror,[8] specified to be a 400 W/Si bi-layer ML with a thickness d of *2.53 nm.* SXR reflectivity spectra of these samples were measured at the PTB beamline at BESSYII, which achieves an energy precision below 0.1 *eV* and a reflectance accuracy of 0.2 %.[9]

Figure 3 shows the measured absolute reflectivity of two LMGs with the same Γ -ratio ($\Gamma = 0.4$) at an SXR energy of 525 *eV*. From Eq. (1) we derived that for single-order operation of these LMGs, the lamel width (ΓD) should be smaller than approximately 200 *nm*, which corresponds to a grating period of *500 nm* for a Γ of 0.4. The first spectrum (violet circles) is from a LMG with grating dimensions $D = 1\ \mu m$ and $\Gamma D = 400\ nm$, while the second spectrum (blue squares) is from an LMG with a small grating period, namely $D = 300\ nm$ and $\Gamma D = 120\ nm$. The third trace (small red stars) is the reflectivity of the unpatterned ML mirror to provide a reference. This reference is slightly shifted in energy due to the higher average polarizability of the individual layers as discussed in Ref. 6.

In the figure, it can be seen that the $D = 300\ nm$ LMG provides increased spectral resolution while this spectrum has no significant side maxima, in contrast to the $D = 1\ \mu m$. At the same time, the $D = 300\ nm$ LMG also has a main Bragg peak which is about a factor of 1.5 higher than the main Bragg peak for the $D = 1\ \mu m$ LMG. Both effects are due to the absence of significant diffraction into higher orders for the $D = 300\ nm$ LMG. Furthermore, the FWHM bandwidth of the $D = 300\ nm$ LMG is a factor of 2.5 narrower than that of the reference spectrum, which is in agreement with the $1/\Gamma$ bandwidth scaling predicted for single-order operating LMGs.[5]

These observations prove that single-order LMG operation can be achieved in the SXR spectral range. The largest resolution improvement, also obtained with a single-order operating LMG around 525 *eV*, had a factor 3.8 narrower bandwidth (1.85 *eV*) than that of the unpatterned ML mirror (7.02 *eV*).

For a more systematic analysis of spectral narrowing in single-order LMG operation, we extended our experiments with reflectivity measurements at a higher photon energy ($E = 1255\ eV$),

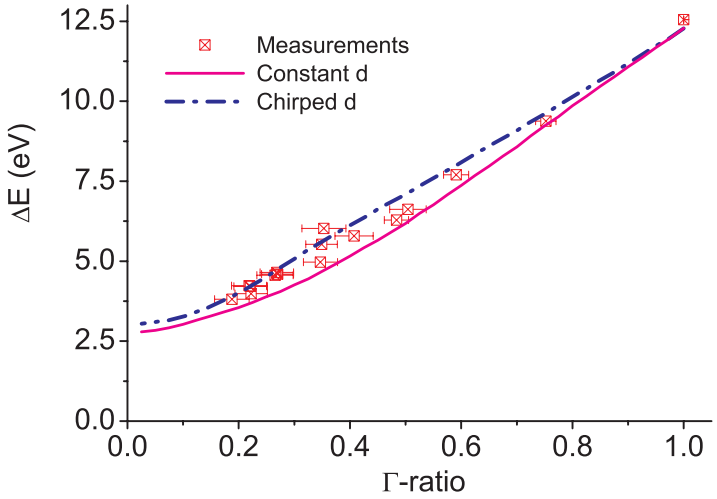

FIG. 4. Measured FWHM bandwidth ΔE for several single-order LMGs at the SXR energy of 1255 eV. Results of calculations using our theoretical model including the measured bi-layer chirp are in good agreement with the measured data.

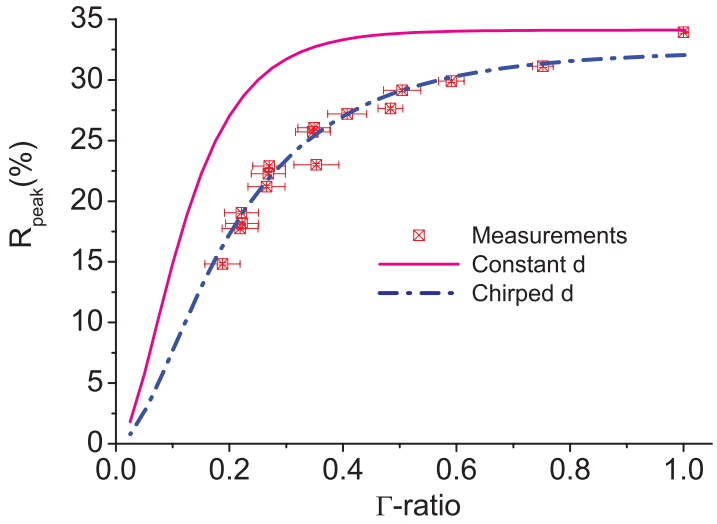

FIG. 5. Measured peak reflectivity (R_{peak}) for several single-order LMGs at the SXR energy of 1255 eV. Results of calculations using our theoretical model including the measured bi-layer chirp are in good agreement with the measured data.

where more LMGs can be operated in the single-order mode for a broader range of Γ values (0.2 to 0.8). The measured spectral bandwidths and peak reflectivities are shown in Figures 4 and 5, respectively, as a function of Γ. It can be seen in Figure 4 that the spectral bandwidth of the LMG decreases with decreasing Γ, showing a factor 3.3 improvement in spectral resolution when going from the unpatterned ML mirror ($\Gamma = 1$) to an LMG with $\Gamma = 0.22$. At the same time, it can be seen from Figure 5 that the peak reflectivity decreases for lower Γ-ratios and drops to approximately half of its initial value at $\Gamma = 0.2$.

We compared the experimental data with theoretical calculations of the spectral bandwidths and peak reflectivities as a function of Γ using our Coupled Waves Approach (CWA).[5,6] In these calculations, we included various effects usually found in ML mirrors, such as rms interlayer roughness (σ) and interface width (w). By fitting the calculations to the measured spectra of the unpatterned ML mirror recorded at various energies and taking the finite number of bi-layers ($N = 400$) into account, we obtained values of $d = 2.53$ *nm*, $\gamma = 0.25$, $\sigma = 0.29$ *nm* and $w = 0.42$ *nm*. These calculations are shown in Figures 4 and 5 as "Constant d". As can be seen, these simulations do not

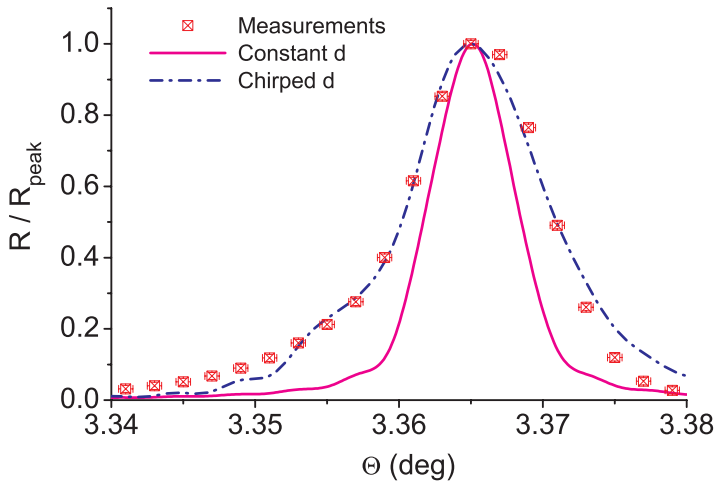

FIG. 6. Normalized second Bragg order of the unpatterned ML measured at the hard x-ray (HXR) energy of 8 *keV*. Comparison with simulations revealed a slight (0.5 %) linear increase (chirp) in the bi-layer spacing d in the depth of the ML.

agree well with the measurements. In particular, the peak reflectivity at lower Γ-ratio's is well below the theoretical value.

Among the possible factors that decrease the peak reflectivity of a ML mirror and, hence, that of a single-order operating LMG, we indicate: (a) interfacial roughness, (b) interlayer formation between neighboring materials due to chemical reactions and interdiffusion, and (c) random or deterministic variation of layers thickness both in the depth and along the ML surface. Although we cannot exclude that the etching of the ML stack could result in increased interfacial roughness or interlayer formation, neither photo-electron spectroscopy data nor high-resolution transmission electron microscopy images indicated any difference between the ML stacks before and after etching. Increased roughness and interlayer formation also only reduce peak reflectivity without increasing the bandwidth. In contrary, simulations showed that layer thickness variations can reduce the peak reflectivity while also increasing reflectivity bandwidths.

As an independent check for bi-layer periodicity, we recorded reflectivity spectra from the Total External Reflection region up to the 4th Bragg order of the unpatterned ML mirror at an X-ray energy of 8 *keV* (HXR). In Figure 6, the normalized 2nd Bragg order is shown and compared to calculations revealing a slight (0.5 %) linear increase (chirp) of the bi-layer thickness d in the depth of the ML stack. Calculations of the SXR spectral bandwidths and peak reflectivities including the measured chirp are shown in Figures 4 and 5 as "Chirped d" and can be seen to agree with the measured data to within a few relative percent. The discrepancy in peak reflectivity between the "Chirped d" simulations and the reference measurement ($\Gamma = 1$) is believed to be caused by sidewall effects that only occur in the LMGs. The reference was actually on the same sample as the LMGs and, as it was therefore exposed to identical fabrication steps as the LMGs, fabrication can largely be excluded as cause for this difference.

Although the bi-layer chirp in the ML stack was not limiting for use as a conventional ML mirror, LMGs require increased accuracies as the SXR penetration depth is increased and the reflected waves thus need to constructively interfere within a narrower bandwidth. To ensure bi-layer thickness variations $\Delta d/d$ are not limiting, they should not exceed $\Delta E/E \approx 1/N_{eff}$ (see Ref. 10 and Refs. therein), leading to the bi-layer thickness accuracy condition:

$$\Delta d_{LMG} \leq \Delta d_{MM}\Gamma \tag{2}$$

where Δd_{LMG} and Δd_{MM} are the tolerable variations in bi-layer thickness for the LMG and conventional ML mirror, respectively.

The agreement of the "Chirped d" simulations with the measurements proves that our modeling adequately describes the main physical effects underlying the measured reflectivity spectra, which

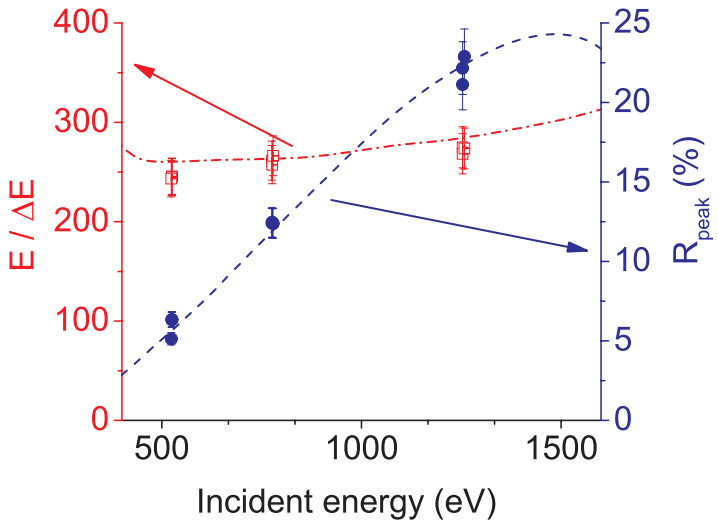

FIG. 7. Measured spectral resolution $E/\Delta E$ and peak reflectivities R_{peak} as function of incident energy for 3 single-order W/Si LMGs with a Γ-ratio of 0.28. The lines are simulations performed assuming the same "Chirped d" values as for Figures 4–6.

is of relevance for systematic improvements in a next experimental step towards further increased resolution and reflection efficiencies, or for an extension to other energies. For instance, the accurate modeling allows us to investigate the usability of LMGs in practical applications by examining the dependence of the spectral resolution $E/\Delta E$ and peak reflectivity on incident energy.

Such a study was performed for our W/Si LMGs as can be seen in Figure 7. Here, measurements are shown of 3 LMGs with Γ-ratios close to 0.28, which are compared to simulations assuming the "Chirped d" values. It can be seen in Figure 7 that the simulations and measurements are in good agreement, which again demonstrates the accurate modeling by our CWA.

The spectral resolution of these LMGs in this energy range can be seen to be between 250-300. For lower Γ-ratios, spectral resolutions of up to 330 were achieved. In comparison, conventional W/Si ML mirrors were previously reported to achieve values of ∼70.[11] However, the usability of LMGs also depends on the peak reflectivity, which has a clear dependence on incident energy. The peak reflectivity can be seen to increase towards higher incident energies with a slight reduction above 1500 *eV*. The changes in peak reflectivity are caused by the energy dependence of the complex refractive index of both materials. Specifically, the absorption reduces when the incident energy increases from 500 to 1500 *eV* resulting in higher peak reflectivities. The slight reduction above 1500 *eV* is due to small variations in the real part of the complex refractive index of tungsten.[12] The usability of LMGs can then be determined by comparing the spectral resolution and peak reflectivity with the requirements for a specific application.

In summary, we have demonstrated the single-order operation of Lamellar Multilayer Gratings (LMG) in the soft x-ray (SXR) spectral range. Their functionality was evident from the absence of any significant diffraction into higher orders and a corresponding increase of the peak reflectivity with respect to a multi-order LMG with the same Γ-ratio. The observed spectral bandwidths and peak reflectivity values are in good agreement with our theoretical model.[5,6] The record value of spectral resolution improvement achieved by single-order operation, which is currently a factor of 3.8 with regard to unpatterned ML mirrors, show the potential of LMGs in single-order operation for many practical applications, such as SXR spectroscopy.

This research is supported by the Dutch Technology Foundation STW, applied science division of NWO and the Technology Program of the Ministry of Economic Affairs. We thank Andrey Yakshin of the FOM Institute DIFFER for performing the HXR measurements.

[1] I. V. Kozhevnikov and A. V. Vinogradov, Phys. Scr. T **17**, 137 (1987).
[2] A. Sammar, M. Ouahabi, R. Barchewitz, J.-M. André, R. Rivoira, C. K. Malek, F. R. Ladan, and P. Guérin, J. Opt. **24**, 37 (1993).
[3] R. Benbalagh, J.-M. André, R. Barchewitz, P. Jonnard, G. Julié, L. Mollard, G. Rolland, C. Rémond, P. Troussel, R. Marmoret, and E. O. Filatova, Nucl. Instr. Meth. Phys. Res. A **541**, 590 (2005).
[4] J.-M. André, R. Benbalagh, R. Barchewitz, M.-F. Ravet, A. Raynal, F. Delmotte, F. Bridou, G. Julié, A. Bosseboeuf, R. Laval, G. Soullie, C. Rémond, and M. Fialin, Appl. Opt. **41**, 239 (2003).
[5] I. V. Kozhevnikov, R. van der Meer, H. M. J. Bastiaens, K.-J. Boller, and F. Bijkerk, Opt. Exp. **18**, 16234 (2010).
[6] I. V. Kozhevnikov, R. van der Meer, H. M. J. Bastiaens, K.-J. Boller, and F. Bijkerk, Opt. Exp. **19**, 9172 (2011).
[7] R. van der Meer, B. Krishnan, I. V. Kozhevnikov, M. J. de Boer, B. Vratzov, H. M. J. Bastiaens, J. Huskens, W. G. van der Wiel, P. E. Hegeman, G. C. S. Brons, K.-J. Boller, and F. Bijkerk, Proc. of SPIE, 8139 (2011).
[8] Xenocs SA, 19, rue Francois Blumet, F-38360 Sassenage, France, www.xenocs.com.
[9] F. Scholze, J. Tümmler, and G. Ulm, Metrologia **40**, S224 (2003).
[10] I. V. Kozhevnikov and A. V. Vinogradov, J. Russ. Las. Res. **16**, 343 (1995).
[11] S. Andreev, A. Akhsakhalyan, M. Bibishkin, N. Chkhalo, S. Gaponov, S. Gusev, E. Kluenkov, K. Prokhorov, N. N. Salashchenko, F. Schafers, and S. Zuev, Cent. Eur. J. Phys. **1**, 191 (2003).
[12] B. L. Henke, E. M. Gullikson, and J. C. Davis, At. Data Nucl. Data Tables **54**, 181 (1993).